

Spectroscopic Properties of the Nonplanar Amide Group: A Computational Study

LUCIE BEDNÁROVÁ,* PETR MALOŇ, AND PETR BOUŘ

Institute of Organic Chemistry and Biochemistry, Academy of Sciences, Flemingovo nám. 2, 16610, Prague 6, Czech Republic

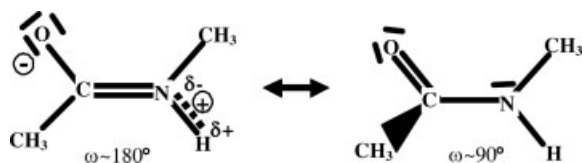
ABSTRACT Experimental studies suggest that amide bond may significantly deviate from planar arrangement even in linear peptides and proteins. In order to find out the extent to which such deviation may influence principal amide spectroscopic properties, we conducted a computational study of nonplanar *N*-methylacetamide (NMA) conformers. Vibrational absorption, Raman, and electronic spectra including optical activity were simulated with ab initio and density functional theory (DFT) methods. According to the results, small nonplanarity deviations may be detectable by nonpolarized spectroscopic techniques, albeit as subtle spectral changes. The optical activity methods, such as the vibrational circular dichroism (VCD), Raman optical activity (ROA), and electronic circular dichroism (CD, ECD), provide enhanced information about the amide nonplanarity, because planar amide is not optically active (chiral). For VCD, however, the inherently chiral contribution in most peptides and proteins most probably provides very weak signal in comparison with other contributions, such as the dipolar coupling. For the electronic CD, the nonplanarity contribution is relatively big and causes a strong CD couplet in the $n-\pi^*$ absorption region accompanied by a red frequency shift. The $\pi-\pi^*$ CD region is relatively unaffected. The ROA spectroscopy appears most promising for the nonplanarity detection and the inherent chiral signal may dominate entire spectral parts. The amide I and III vibrational ROA bands are most challenging experimentally because of their relatively weak coupling to other peptide vibrations. *Chirality* 19:775–786, 2007. © 2007 Wiley-Liss, Inc.

KEY WORDS: nonplanar amide bond; peptide geometry; proteins; spectroscopy; circular dichroism; vibrational optical activity; Raman scattering; *N*-methylacetamide

INTRODUCTION

As the methods of structural biology develop, new properties and structural details of proteins become accessible to systematic investigations. Geometry of the amide group represents a typical example of such gradual refinement. The amide group is an important building block of peptides and proteins and it is embedded in many molecules of fundamental importance for living matter, industry and general chemistry. The amide chromophore is rather small, but its complex electronic structure involves a carbon–oxygen double bond, a carbon–nitrogen partial double bond, three center π -system, and three lone electrons pairs. Historically, the amide linkage was considered planar and fairly rigid, based on the original ideas of Pauling about a partial double $C'-N$ bond character which is disturbed by the nonplanarity:¹

This approximation allowed explaining principal features of protein structure, especially for conformations such as α -helices or β -sheets. However, at the seventies, semiempirical calculations and X-ray studies indicated slightly nonplanar amide groups for small cyclic peptides² or medium ring lactams³ exhibiting ring constraints. These results were confirmed by resolving crystal structures of many small peptides³ and set upper bounds of $\sim \pm 5^\circ$ deviation of the backbone angle ω from either cis ($\omega = 0^\circ$) or trans ($\omega = 180^\circ$) planarity in linear peptides. Later, more profound distortions were observed in NMR and X-ray studies.^{4,5} Finally, as structural databases became more complete and reliable, statistical works revealed significant and systematic deviations from planarity of the trans-like



© 2007 Wiley-Liss, Inc.

Contract grant sponsor: Grant Agency of the Czech Republic; Contract grant numbers: 203/06/0420, 202/07/0732; Contract grant sponsor: Grant Agency of Academy of Sciences; Contract grant number: A400550702.

*Correspondence to: Lucie Bednárová, Institute of Organic Chemistry and Biochemistry, Academy of Sciences, Flemingovo nám. 2, 16610, Prague 6, Czech Republic. E-mail: bednarova@uochb.cas.cz

Received for publication 17 April 2007; Accepted 3 July 2007

DOI: 10.1002/chir.20462

Published online 8 August 2007 in Wiley InterScience (www.interscience.wiley.com).

peptide bond (with ω close to 180°) in most peptide and protein structures.^{6–8} For example, MacArthur et al.⁶ observed average nonplanarity deviations of about 6° for cyclic and linear peptides. Consequent analysis of a data set of 187 proteins provided an average deviation of 4.7° . On average, the amide groups thus were chiral. The angle ω depends on protein secondary structure, especially the α/β conformer ratio, and on peptide side chains. Later, X-ray protein data of atomic resolution provided even bigger deviations, up to 20° .^{8–11} Except for the importance for peptide folding and secondary structure, the amide nonplanarity also influences reactivity of hydrolytic reactions¹² or susceptibility to nucleophilic attacks.¹³

The distortion from the planarity is most often characterized by the main chain torsion angle ω . However such a simple rotation does not describe amide nonplanarity in full, because it involves also pyramidal out-of-plane deviations on carbonyl carbon and especially nitrogen atoms as has been described already by Ramachandran and co-workers.^{14,15} The relevant pyramidity descriptors χ_N and χ_C (Fig. 1) were introduced by Warshel¹⁶ and elaborated further by Winkler and Dunitz.³ The bonds-to-nitrogen out-of-plane deformation can be quite large and for trans-like amides it approximately correlates with the ω parameter by $\chi_N \approx -2\Delta\omega$, where $\Delta\omega = \omega - 180^\circ$.^{6,17,18} The pyramid on carbonyl carbon is smaller and the observed distortions rarely exceed 5° .^{19,20} A correlation was observed of the sense of nonplanar deformation with the handedness of proteins main chain twist.⁶

Optical spectroscopies and theoretical calculations often complement crystallographic investigations of the amide nonplanarity.^{21,22–25} The spectroscopic techniques usually yield lower resolution, but allow for studies of solutions. Especially the dichroic methods are very convenient for nonplanarity studies as the loss of the amide symmetry plane

leads to the inherently chiral chromophore. Infrared absorption and electronic circular dichroism (ECD) of significantly nonplanar ($\omega = 10\text{--}15^\circ$) cis-like amide groups in rigid polycyclic lactams were already analyzed empirically, and with the aid of CNDO and HF calculations.^{26–28} CD signal originating in the nonplanarity was found quite large ($\Delta\epsilon \sim 10 \text{ l mol}^{-1} \text{ cm}^{-1}$), the $n\text{--}\pi^*$ band red shifted, and the $n\text{--}\pi^*/\pi\text{--}\pi^*$ dichroic intensity ratio increased (typically from 1/3 to 1/1 for the planar and nonplanar chromophores).^{26,28–30} IR spectra indicated a correlation of the nonplanarity magnitude with amide I and amide II frequencies,^{26,27} which was also supported by theoretical studies.^{31,32}

Newer vibrational optical activity techniques appear convenient for the amide nonplanarity studies, similarly as ECD. Particularly, the vibrational circular dichroism (VCD)^{33–35} and the Raman optical activity (ROA)^{36,37} provided priceless data about peptide and protein geometry. Conveniently, the vibrational molecular properties depend on the electronic ground state and can be normally calculated with better precision than with ECD. The relatively local vibrational normal modes are also more attentive to structural details. Nevertheless, vibrational studies of the nonplanarity are rather rare. The amide twist was related to the CD bands for polycyclic lactams.^{29,30,32} A significant nonplanarity contribution to the VCD of an α -helical peptide segment was predicted.³⁸

In this study, we compare various spectroscopic properties of the nonplanar amide chromophore represented by a distorted *N*-methylacetamide (NMA) to mimic the behavior of amide groups in peptides on the basis of experimental spectroscopy and theoretical calculations.^{38,39} The emphasis is put on possible effects in protein and peptide spectra, where the nonplanarity is much smaller than in strained lactams and similar rigid compounds. Such theoretical studies based on accurate computations of small peptide bond models proved to be beneficial in the past.^{14,15,31,40,41} Vacuum equilibrium NMA conformers are nonplanar themselves and their energies and VCD and ROA spectra are discussed in Ref. 39. In our model, the methyl rotation and all the other geometrical parameters are allowed to relax fully, while the angle ω is chosen as the varied coordinate. We scanned the ω angle over the full range $0\text{--}180^\circ$ and discuss the potential energy surface (PES) and spectroscopic molecular properties. We looked more closely on the dependence of spectral properties on smaller deviations from the trans ($\omega = 180^\circ$) planar arrangement in order to estimate effect of nonplanarity on real spectra of peptides or proteins. The coupling and the spectral effects of the ω -distorsion to the χ_N and χ_C parameters³ are discussed on the basis of two-dimensional PESs.

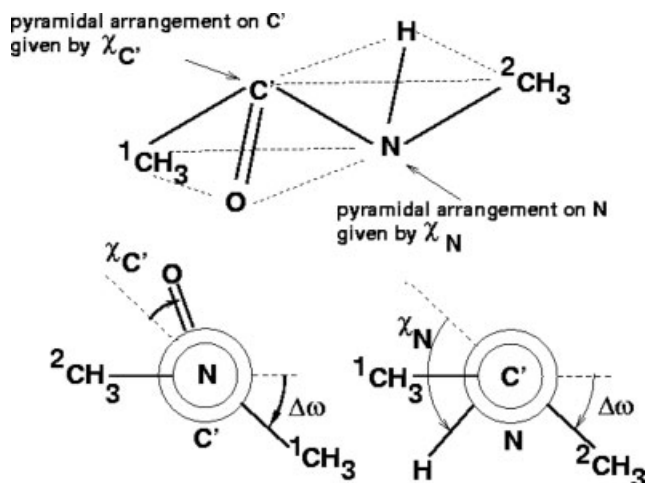


Fig. 1. The usual amide group nonplanarity parameters. The dihedral angles χ_C and χ_N are defined as $\chi_C = \omega_1 - \omega_3 + \pi \pmod{2\pi} = -\omega_2 + \omega_4 + \pi \pmod{2\pi}$ and $\chi_N = \omega_2 - \omega_3 + \pi \pmod{2\pi} = -\omega_1 + \omega_4 + \pi \pmod{2\pi}$, where ω_i are the torsion angles $\omega_1 = \omega = \angle(\text{}^1\text{C C}'\text{N } ^2\text{C})$, $\omega_2 = \angle(\text{O C}'\text{N H})$, $\omega_3 = \angle(\text{O C}'\text{N } ^2\text{C})$, $\omega_4 = \angle(\text{}^1\text{C C}'\text{N H})$; $\Delta\omega = \omega - 180^\circ$. The angles ω_1 , ω_2 , ω_3 , and ω_4 are additionally coupled by $(\omega_1 + \omega_2) - (\omega_3 + \omega_4) = 0 \pmod{2\pi}$.^{14,15}

METHODS

The Gaussian program⁴² was used for the scans of PES and spectral simulations of the NMA molecule. By default, the DFT B3LYP functional⁴³ and 6-311++G** basis set was applied. Other functionals (BPW91, B3PW91⁴⁴) and alternative quantum chemical methods (HF, MP2⁴⁵) with the 6-311G** and 6-311++G** basis sets were tried for

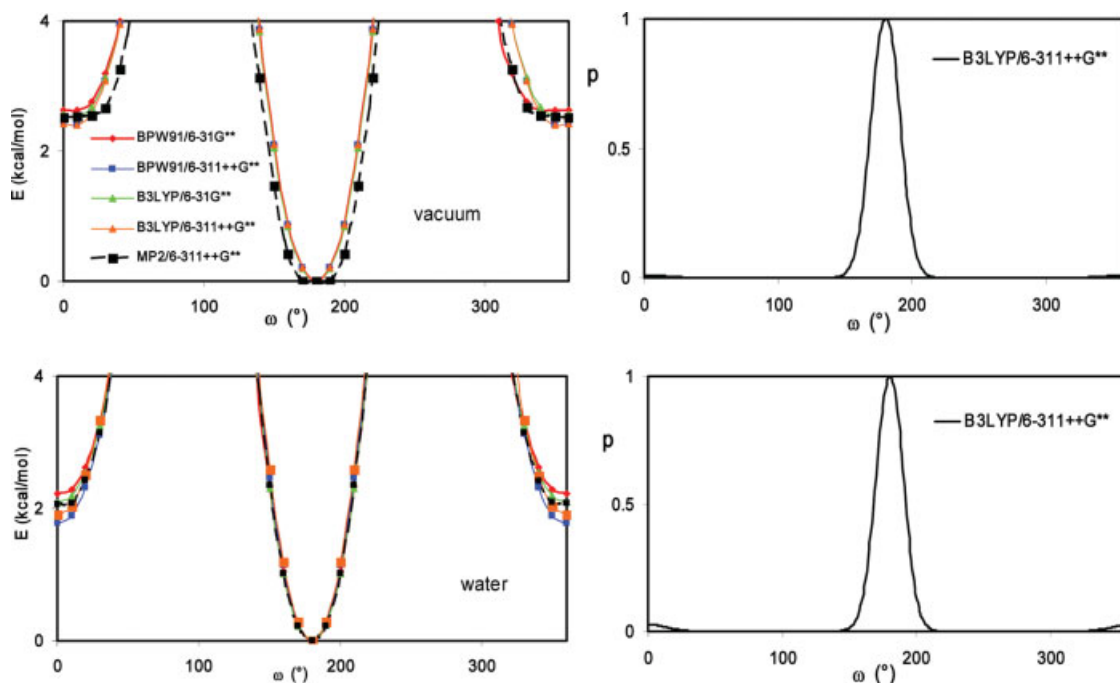


Fig. 2. Calculated dependence of the NMA relative energy on the torsion angle ω as calculated by the five approximation levels in vacuum (top) and with the implicit solvent model (bottom, CPCM). At the right hand side, corresponding Boltzmann probabilities at 300 K for the B3LYP/6-311++G** method are plotted. [Color figure can be viewed in the online issue, which is available at www.interscience.wiley.com.]

control computations. In order to approach usual experimental conditions the aqueous environment was simulated with the CPCM Gaussian variant of the COSMO continuum solvent model. Within all potential energy scans (ω , χ_N , χ_C) the remaining coordinates were allowed to relax fully. In the ω -scans, we neglected a hysteresis in the PES which occurs around $\omega \sim 90^\circ$. This region is not relevant for most peptides and this hysteresis is caused by a simultaneous methyl group rotation and inversion at the nitrogen atom. For selected geometries infrared absorption, VCD, Raman, ROA, and ECD spectra were simulated with our complementary programs.^{46–48} An arbitrary bandwidth of 5 cm^{-1} and 5 nm was used for the vibrational and electronic spectra simulation, respectively. The back-scattered ICP Raman and ROA experiment was modeled. The harmonic approximation and gauge-independent atomic orbitals (GIAO) were used for the VCD⁴⁹ and ROA simulations.⁵⁰ ECD spectra were calculated with the time-dependent density functional theory (TDDFT).⁵¹

RESULTS AND DISCUSSION

Amide Geometry and Flexibility

Using NMA as a model implies that the dependency of NMA energy on the ω angle can be approximately extrapolated to amide bonds in peptides and proteins. As can be seen in Figure 2 various approximation levels provide consistent energy profiles. Almost identical dependence of the relative energy on the angle ω was obtained with the BPW91 and B3LYP functionals, with minor differences for the 6-31G** and 6-311++G** bases. Only in vacuum both

the cis and trans minima at MP2 level are slightly broader than in the case of DFT methods. However, in water, the MP2 and DFT results almost coincide for $\omega \sim 180^\circ$. Solution cis/trans transition barriers (not visible in the plots) differ more for various levels than in vacuum, but were obtained in a very narrow range by all the methods, within 17.6–18.6 and 19.2–20.6 kcal/mol in vacuum and water, respectively. Similar values were found previously.⁵² The trans conformer is clearly energetically favored, although residual population of the cis states is apparent in the probability graphs at the right-hand side of the figure, more for the aqueous environment. Around the trans isomer minimum the angle ω can vary relatively freely at 300 K, according to the probability distribution half width within $\sim 166^\circ$ – 194° for vacuum and slightly less ($\sim 168^\circ$ – 192°) in water. Also this behavior corresponds, for example, to the results of Rick and Cachau,⁴⁰ who estimated distribution of the ω -angles for protein structures from molecular dynamic simulations. An analysis of the protein structure PDB database provided similar values.⁶ This comparison suggests, in accord with the work of others,^{14,15,31,41} that minor nonplanarity in peptide units is quite frequent. It is moderated by peptide side chains, secondary structure, and molecular environment. In NMA, a recent computational analysis by Polavarapu et al.³⁹ revealed that slightly nonplanar conformers ($\Delta\omega \sim 5$ – 8°) represent the only true minima on the PES.

The variation of ω is accompanied by changes of the χ_N and χ_C angles. As follows from Figure 3, the pyramidity on the amide nitrogen is quite strongly coupled to the ω angle, while the χ_C angle deviates only slightly from zero. A more detailed coupling pattern can be seen in the two-dimensional potential energy plots (Fig. 4). From the plots

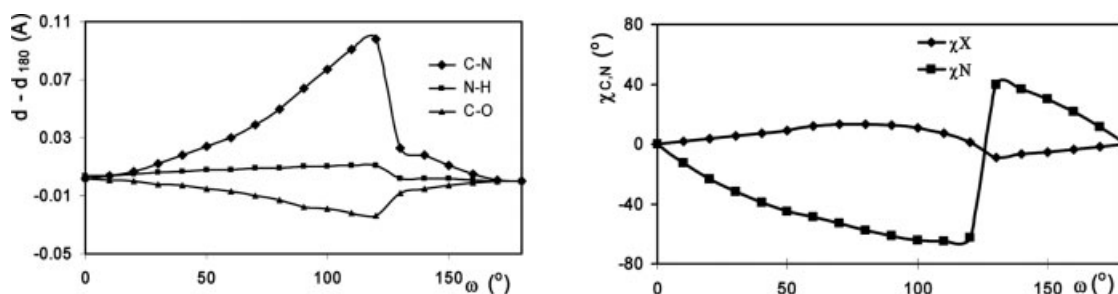


Fig. 3. Computed (B3LYP/CMCP/6-311++G**) changes of selected NMA bond lengths (d) as functions of the angle ω , related to $\omega = 180^\circ$. The reference equilibrium values (planar amide) for the three bonds were 1.348 Å (C–N), 1.020 Å (N–H), and 1.238 Å (C=O) (left). Simultaneous changes of the dihedral angles χ_C and χ_N (Fig. 1) are plotted on the right-hand side.

showing the vicinity of the potential well, we can also see that the χ_N coordinate is strongly correlated to ω in contrast to the χ_C angle. The equilibrium is located at the planar arrangement, but the amide hydrogen and oxygen atoms can easily move out of the plane. The nitrogen pyramidity χ_N occurs more easily. We can estimate that at room temperature (Boltzmann quantum $kT \sim 0.6$ kcal/mol) the angles oscillate from the planar arrangement up to about 8° and 20° for χ_C and χ_N , respectively. In addition to the modification of bond arrangement on amide C' and N atoms the ω -deformation causes changes of the C–N, N–H, and C=O bond lengths (Fig. 3). The equilibrium values for the three bonds are approximately in agreement with previous HF calculation,³¹ and *ab initio* simulations with an alternative IEF solvent model,⁵³ as well as with MD studies.⁵⁴ As can be seen in Figure 3, the C–N bond is prolonged most and the C=O bond is shortened during the ω rotation. The changes can be explained on the basis of the amide π -electron system. The system is weakened for nonplanar conformations and the electrons move to the C=O bond that becomes stronger. As pointed out previously, the weakening of the C–N bonds is directly related to magnitude of nonplanarity.⁴¹ The weakening of the N–H bond with the ω -twist seems to be minor, but it has an effect on N–H stretching frequencies (see below).

Vibrational Absorption and Vibrational Optical Activity

The dependence of amide A, I, II, and III vibrational frequencies on the ω -rotation is shown in Figure 5. The calculated frequencies for the planar trans arrangement ($\omega = 180^\circ$) are compared with experimental values in Table 1. The frequencies are rather sensitive to nonplanar distortion. The amide A frequency shifts the most, which

indicates that the N–H bond is very weakened. The maximum frequency change of -175 cm^{-1} for $\omega \sim 100^\circ$ is somewhat moderated by the aqueous environment. Calculated N–H stretching frequencies are lower for the cis form (3617 cm^{-1} in vacuum (v), 3321 cm^{-1} in water (w)) than for the trans conformer (3643 cm^{-1} (v), 3363 cm^{-1} (w)). On the contrary, the amide I (C=O stretching) frequency rises when the amide group becomes nonplanar and in the vicinity of $\omega \sim 90^\circ$ it approaches values characteristic for ketones. It is interesting, that sensitivity of this vibrational mode to a small ω -change appears bigger for the trans than for the cis conformer. Unlike for amide A, the solvent makes the amide I frequency more susceptible to the ω -changes; however, vacuum amide I frequencies of planar trans and cis forms differ from one another more than in water (cf. Table 1). The amide II and III frequencies of the cis and trans forms significantly differ, too, and the difference is emphasized by the aqueous environment. This indicates, that not only the change of ω , but also the cis/trans isomerization leads to a significant modification of amide electronic structure. Therefore, in vibrational spectroscopy, there is an important difference between cis- and trans-like amides, and consequently rigid polycyclic lactams which serve as nonplanar amide models in electronic spectroscopy^{27–30} should be used for IR modeling only with great caution. Around $\omega = 180^\circ$, the amide II frequency appears more sensitive to small ω -changes than that of amide III mode. Band intensities are even more sensitive to nonplanarity than vibrational frequencies (see Fig. 6, where the amide intensities are plotted relative to planar trans arrangement). Clearly, intensity variations can exceed 100% for both absorption and Raman scattering. As an extreme case, the Raman amide II intensity is four

TABLE 1. Comparison of calculated (B3LYP/6-311++G**) NMA harmonic frequencies (cm^{-1}) of the amide A, I, II, and III normal modes with experimental values for aqueous solutions

	Amide A ($\nu(\text{NH})$)	Amide I ($\nu(\text{C}=\text{O})$)	Amide II ($\nu(\text{C}-\text{N})$, NH bend)	Amide III ($\nu(\text{C}-\text{N})$, NH bend)
Vacuum-cis	3617	1749	1522	1343
Vacuum-trans	3643	1744	1559	1265
Water-cis	3321	1649	1513	1357
Water-trans	3363	1651	1584	1302
Exp ^{63–67}		1617	1577	1314
		1620	1580	1315
		1625	1582	

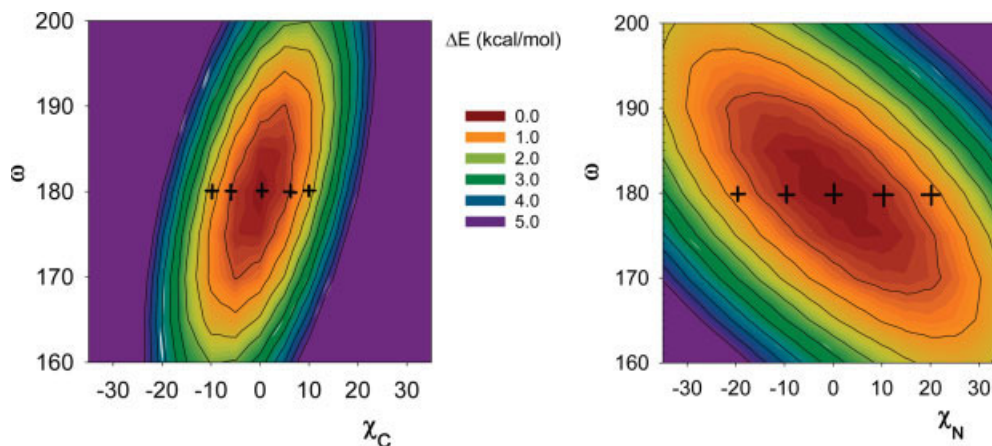


Fig. 4. NMA PESs (B3LYP/6-311++G**/CPCM, with isolines each 0.5 kcal/mol) showing the coupling of the ω -twist with the χ_C and χ_N Winkler³ angles (Fig. 1). The crosses denote geometries chosen for the spectra calculations ($\chi_C = 0^\circ, \pm 5^\circ, \pm 10^\circ$ and $\chi_N = 0^\circ, \pm 10^\circ, \pm 20^\circ$). [Color figure can be viewed in the online issue, which is available at www.interscience.wiley.com.]

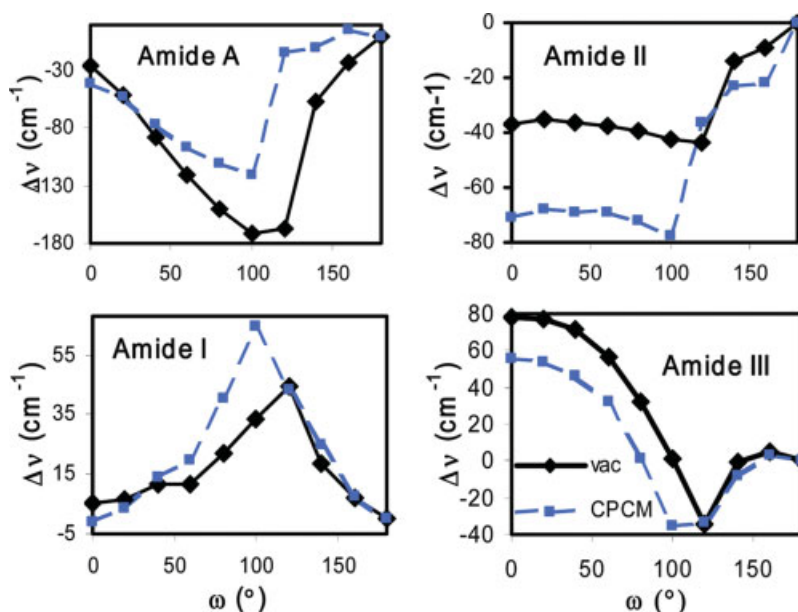


Fig. 5. Dependencies of the harmonic frequencies of the amide group vibrational normal modes on the ω -angle calculated by the B3LYP/CMCP/6-311++G** method (changes with respect to the trans ($\omega = 180^\circ$) conformation are plotted). [Color figure can be viewed in the online issue, which is available at www.interscience.wiley.com.]

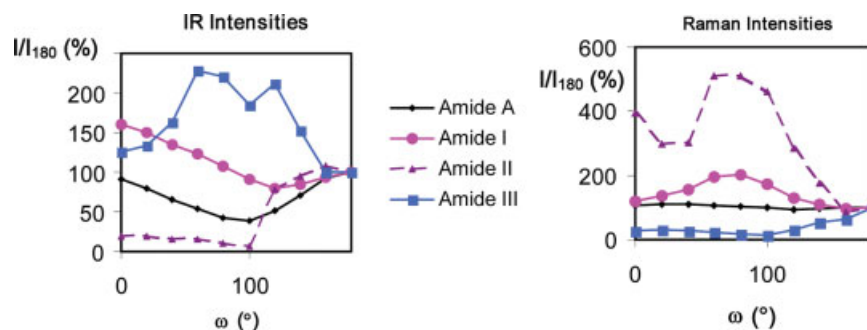


Fig. 6. Relative IR and Raman intensity changes with respect to the trans conformation (B3LYP/CPCM/6-311++G** calculation). [Color figure can be viewed in the online issue, which is available at www.interscience.wiley.com.]

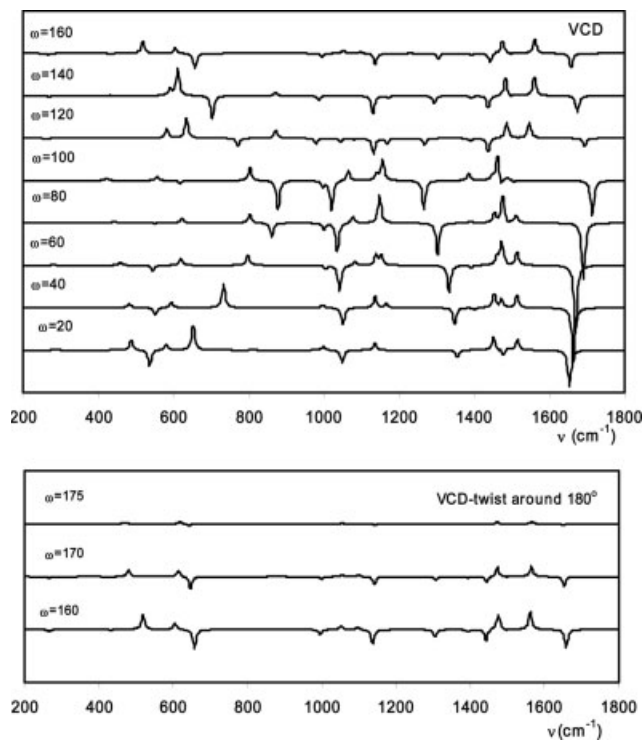


Fig. 7. Calculated (B3LYP/PCM/6-311++G**) VCD intensities for selected NMA conformers. Spectra for twists around 180° are plotted on the bottom separate panel.

times bigger for the cis form than for the trans conformer; for ω -values around 90° even a difference of more than 500% is predicted. This can be explained by coupling of the amide II and amide III vibrations to other vibrational modes, particularly to those associated with polarizable methyl groups.

Chiral spectroscopies provide a more direct way to investigate the amide nonplanarity than the IR absorption or Raman scattering as the nonplanar amide bond is chiral. Investigation of a model compound like NMA should provide sign assignments of amide VOA bands to particular amide chirality. In Figure 7 VCD and in Figure 8 backscattered ROA spectra are simulated for nonplanar NMA structures. In VCD the amide I band ($1649\text{--}1715\text{ cm}^{-1}$) is uniformly negative for $0^\circ < \omega < 180^\circ$, while amide II ($1506\text{--}1584\text{ cm}^{-1}$) is uniformly positive and amide III band ($1267\text{--}1367\text{ cm}^{-1}$) again negative. The predicted VCD signals are quite intense for all three vibration types (either stronger or similar in intensity as the VCD connected with CH_3 deformation modes, $1400\text{--}1490\text{ cm}^{-1}$). These bands would be opposite for negative values of ω ($0^\circ > \omega > -180^\circ$). The circularly polarized IR light probes amide chirality as directly related to the sense of ω , while the VCD bands related to C–H deformations ($1400\text{--}1490\text{ cm}^{-1}$) depend on the ω angle in a more complicated way. A similar trend is observed in ROA spectra, however the corresponding ROA signals are less intense, and the trend is less convincing: amide I vibration exhibits positive ROA for $0^\circ < \omega < 180^\circ$ however there is a temporary sign flip

Chirality DOI 10.1002/chir

around $\omega \sim 100^\circ$. The amide II and III ROA signals in the vicinity of the more intense CH_3 rocking modes are quite weak. The amide I, II, III VCD and ROA bands exhibit significant position and magnitude changes for ω in the range $0\text{--}180^\circ$. At $\omega \sim 100^\circ$ the amide I VCD band is shifted to $\sim 1720\text{ cm}^{-1}$ (ketone-like value, indicating complete decoupling from the rest of amide grouping) and accompanied by the sign flip in the ROA spectrum. The maximum of IR absorption occurs earlier, at $\omega = 60^\circ$ (Fig. 5). We have also simulated VCD spectral changes caused by different pyramidal arrangements with $\chi_C = 0^\circ, -5^\circ, -10^\circ$ and $\chi_N = 0^\circ, -10^\circ, -20^\circ$ for $\omega = 180^\circ$, marked by the crosses at the PES maps in Figure 4. The intensity changes in the spectra caused by these deformations can be seen in Figure 9. They are comparable in magnitudes to those given in Figures 7 and 8. Note, that $\chi_N \approx -\Delta\omega$. As the relative intensity ratios are different for different transitions the effects caused by χ_N and χ_C can thus intensify or cancel the ω -twist effects. In ROA, the χ_N change leads to different signs of the amide I and II contributions. Thus the effect of the pyramids should be taken into account in interpreting spectra of complex peptides.

If we put particular emphasis on most relevant geometries for real peptides and proteins (trans-like amide and slight deviations like, e.g. $\omega \sim 170^\circ$, i.e. $\Delta\omega \sim -10^\circ$), we can deduce that for the given chirality the amide I signal is predicted to be slightly blue shifted and negative in VCD, while in ROA it would be positive. Amide II fre-

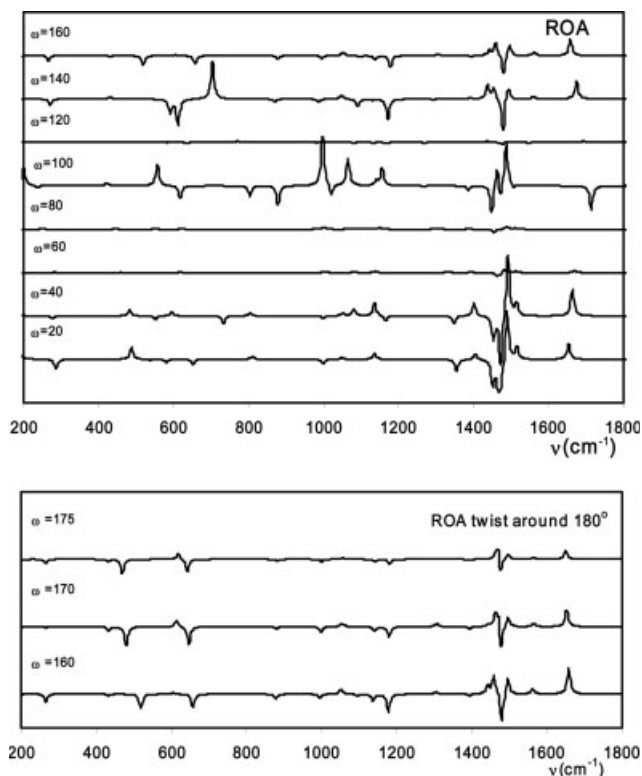


Fig. 8. Calculated (B3LYP/PCM/6-311++G**) ROA intensities for selected NMA conformers. Spectra for twists around 180° are plotted at the bottom.

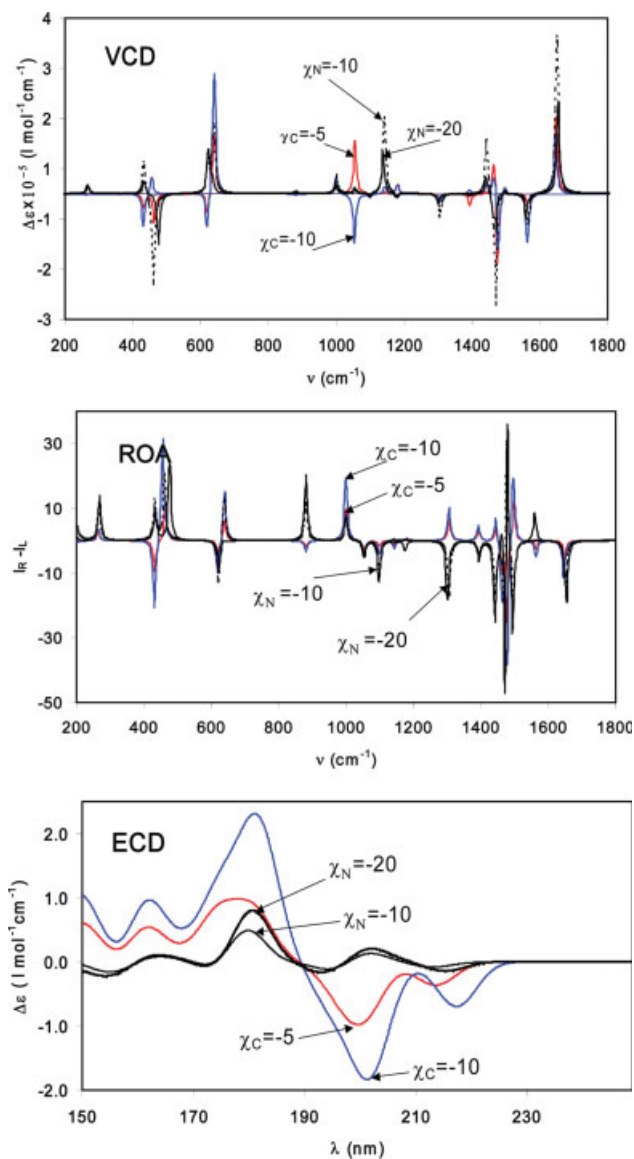


Fig. 9. Calculated VCD, ROA, and ECD spectra for NMA conformers with selected pyramidal deformations for geometries defined in Figure 4. [Color figure can be viewed in the online issue, which is available at www.interscience.wiley.com.]

quency shifts slightly to the red, and the signal is positive in both techniques (though it is weaker in ROA). According to previous studies, $\chi_N \approx -2\Delta\omega$,^{14,15} such enhanced pyramidal arrangement leads to a further increase in the magnitude of VCD and ROA signals of amide I and II. The changes in the amide III region are more complex, partially because of the coupling with the methyl hydrogen bending motion. Additionally, in real peptides, the chirality on the alpha-carbon causes an additional contribution, since the C–H bending motion is strongly coupled with the amide III vibration.

The spectral region below 1000 cm^{-1} is experimentally difficult for VCD, but should be easier to reach by the Raman and ROA techniques. For the nonplanarity detec-

tion, this is convenient because the amide IV (around 880 and 640 cm^{-1}) and amide V (620 and 460 cm^{-1}) vibrations directly probe the respective amide C=O and N–H out-of-plane bending motions. Figures 7 and 8 show the results of our calculations in this spectral region and the most important case of small trans-like nonplanarity. The VCD signal predicted at this region is also significant, but very difficult to measure. However, the ROA signals are quite characteristic and might help in the nonplanarity detection and its sense assignment. For $\Delta\omega \sim -5$ to -10° , the 880 cm^{-1} ROA is negative, while the signals at 620 and 640 cm^{-1} form a positive–negative couplet. The calculated amide V signal at $\sim 470\text{ cm}^{-1}$ is negative. Our calculations are in agreement with the results of Polavarapu et al.³⁹ where the spectra were simulated for the opposite chirality. Therefore ROA signs therein have to be flipped for comparison with our calculations. Similarly, the VCD signs also agree with the exception of the band $\sim 470\text{ cm}^{-1}$.

Electronic Absorption and ECD

Changes in the electronic absorption and CD spectra caused by nonplanarity can be seen in Figures 9 and 10. They are more distinct than the vibrational alterations as the electronic bands more directly probe the $sp^2 \rightarrow sp^3$ hybridization change. Historically, electronic spectra of the amide group were considered as a composition of $n-\pi^*$ (210 – 250 nm) and $\pi-\pi^*$ (180 – 200 nm) absorption bands, both originating from the amide π -electron system and amide lone electron pairs. The $n-\pi^*$ transition, which is detectable in absorption only as a small shoulder on the $\pi-\pi^*$ dominant band, is clearly visible in ECD. The $\pi-\pi^*$ transition dominates both the absorption and CD. However, we calculated additional absorption and associated CD bands in addition to these two transitions. Such additional bands have been calculated before in the spectra of small amides^{55,56} or observed experimentally in the spectra of polycyclic rigid optically active lactams.^{28,29} These bands have been ascribed either to Rydberg type transitions^{55–57} or to a vibronic fine structure within the $n-\pi^*$ band. In our spectra these bands originates from the methyl groups. They are of $\pi-\sigma^*$ or $n-\sigma^*$ type and they occur exclusively within the valence electron shell (our basis set does not include Rydberg type orbitals).

In our calculations (Fig. 10), we can distinguish three regions of ω angle: in the vicinity of either cis or trans planar arrangement, characterized by minor deformations where the nonplanarity induced electronic changes remain minor and quantitative (they may be observed mainly by induced band shifts and CD), and the area around $\omega = 90^\circ$ which is characterized by more qualitative electronic changes. For the latter arrangement we observe an extreme red shift of the $n-\pi^*$ band (up to 280 nm) and a second $n-\pi^*$ band (from the nitrogen lone pair) appears at 210 nm . For $\omega \sim 90^\circ$, CD $n-\pi^*$ intensity is lower than for smaller deformations, because at such geometry amide chromophore (CON) has again a plane of symmetry and is therefore not inherently chiral and the observed CD comes from neighboring atoms. These results although extreme for peptides and proteins are quite real and have been experimentally realized in lactams having quinucli-

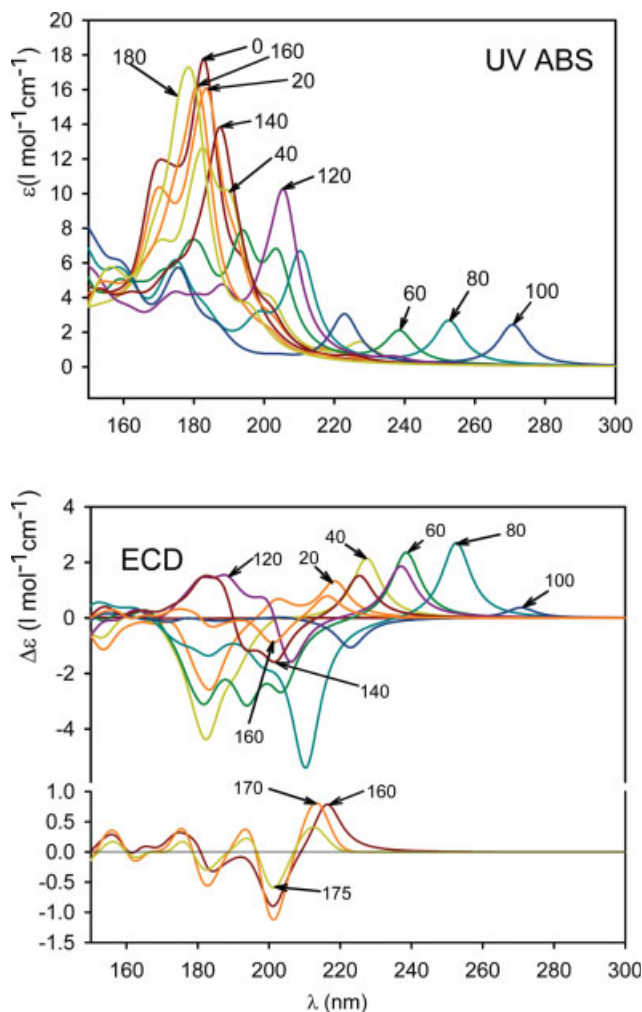


Fig. 10. Calculated (TD DFT B3LYP/CMCP/6-311++G**) absorption (top) and ECD (bottom) spectra for twisted NMA conformers. [Color figure can be viewed in the online issue, which is available at www.interscience.wiley.com.]

done skeleton which behave like amino ketones.⁵⁸ Minor amide deformations that do not mean a qualitative chromophoric change are still quite discernible on the basis of ECD spectroscopy. The global maximum of the π - π^* band is also shifted to higher wavelengths for nonplanar structures. Its CD signs correlate with the sense of amide deformations and together with spectral shifts they are in a good coincidence with previous studies of amide bond nonplanarity based on cis-like rigid cyclic lactams.^{29–31} These phenomena have useful diagnostic value for the ECD detection of nonplanar amides.

The electronic redistribution caused by slight nonplanarity causes rather complex changes in the ECD spectra. A simple interpretation using mixing of the n - π^* and π - π^* configurations leads to a couplet, where the n - π^* state loses its pure n - π^* character and vice versa. This complexity can be qualitatively estimated also from the orbital changes as shown in Figure 9. The n (HOMO) orbital loses some nodal planes perpendicular to the amide plane in twisted amide. The n electronic density also par-

tially escapes from the oxygen lone pair lobes for $\omega = 170^\circ$. These changes are probably responsible for the bigger sensitivity of the n - π^* signal to geometry changes. But also π and π^* (LUMO) orbitals seem to be affected; π^* is even losing the amide nodal plane around the methyl group on the right-hand side in Figure 11. This could be formally described using the Sznatzke formalism.⁵⁹ The absolute CD signs relate to relative orientations of the carbonyl group and the nitrogen lone pair. Since this is independent of cis/trans amide isomerism then at this level of approximation ECD should be independent of cis/trans configuration as well and, consequently, model experiments based on cis-like polycyclic lactams should be transferable to *trans*-amide groups in peptides and proteins. However our more detailed calculations do not fully support such an interpretation as they cast some doubts on the π - π^* nature of the short wavelength dominant band. In fact, for *trans*-like amides it seems that the dominant band is mostly formed by π - σ^* and n - σ^* components and that the π - π^* band has hardly any CD intensity.

The transitions contributing to n - π^* bands split and provide a double-signed pattern within 195–225 nm for $\omega = 180$ – 160° . The values of ω closer to 180° are the most important for practical ECD spectroscopy and simulations thus suggest that especially signal of α -helical peptides (with the biggest propensity to systematic nonplanar amides) may be moderated by this internal chirality contribution. The oscillatory π - π^* CD signal at lower wavelengths would be difficult to separate from other contributions in real peptides. The changes in ECD spectra caused by χ_N and χ_C can be seen in Figure 9 and they are also complex. Significantly bigger signal can be caused in the π - π^* region (~ 180 nm) by χ_C than by χ_N or ω deformations.

Experimental Aspects

In principle, the spectral changes caused by nonplanar deviations observed for proteins are rather significant and should be taken into account when interpreting experimental data. It is even possible that some features of chiroptical spectra of well-recognized standard peptide/protein structures are contributed by nonplanarity issues. To evaluate usefulness of particular chiroptical methods for the detection of amide nonplanarity, one has to consider several aspects: ECD is easy to measure and very sensitive to small variations of molecular three-dimensional structure. Nonplanarity would most unequivocally show up within the n - π^* ECD band, which is calculated to be very well sign-correlated to the amide chirality and bathochromically (red) shifted for nonplanar situation. The respective ECD intensity changes caused by realistic nitrogen (χ_N) or carbon (χ_C) deformations make up to about 10% and 50% of usual peptide and protein CD intensities.⁶⁰ Thus standard ω deviations reported in the literature⁶ (about 6° , in some cases^{11,61} to 15 – 20°) are not negligible for the spectra and should be considered in the modeling. ECD is however strongly influenced by long distance interchromophoric coupling, which can obscure the nonplanarity signal for small deviations. The detailed ECD study is currently difficult as the available ab initio simula-

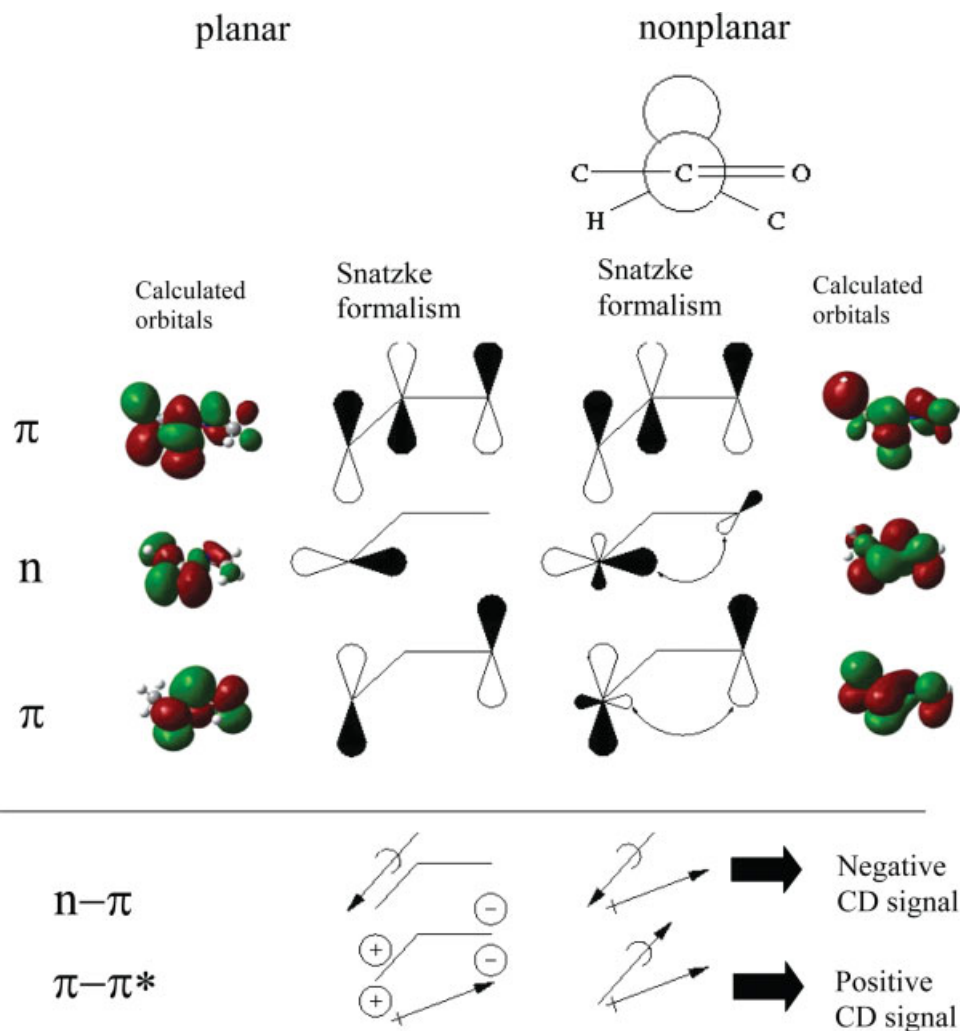


Fig. 11. Calculated molecular orbitals for planar and nonplanar (170°) NMA and their schematic explanation by the Sznatzke formalism.⁵⁹ [Color figure can be viewed in the online issue, which is available at www.interscience.wiley.com.]

tion techniques, including TDDFT, have limited precision and they are restricted by size of the systems. Also the role of the molecular flexibility and solvent⁶² is poorly understood and can interfere with the nonplanarity signal. Obviously, the nonplanarity contributions can be further averaged by temperature motion and protein dynamics. Nevertheless, ECD can be certainly used as a quick and simple experiment for nonplanarity indication.

The vibrational spectra provide more local geometry information and are more convenient for the nonplanarity detection. The VCD and especially the ROA technique also appear to be able to distinguish the carbon (χ_C) and nitrogen (χ_N) pyramidalicity. However, the amide I band is broadened by interactions with the aqueous environment and strongly influenced by dipole-dipole interactions in real proteins. The same argument is valid for amide I

TABLE 2. Calculated VCD and ROA *G*-factors (ratios of the difference and total signal) for amide I and III bands for selected NMA conformers

	$\chi_C = 5^\circ$	$\chi_C = 10^\circ$	$\chi_N = 10^\circ$	$\chi_N = 20^\circ$	$\omega = 175^\circ$	$\omega = 170^\circ$	Exp
Amide I							
VCD	1.9×10^{-6}	8.0×10^{-7}	2.2×10^{-6}	4.0×10^{-6}	-6.4×10^{-7}	-1.3×10^{-6}	5.0×10^{-4}
ROA	-3.5×10^{-4}	-9.0×10^{-4}	-1.0×10^{-3}	-1.2×10^{-3}	1.0×10^{-3}	1.9×10^{-3}	-1.4×10^{-4}
Amide III							
VCD	-1.6×10^{-7}	-7.6×10^{-7}	-1.9×10^{-6}	-2.2×10^{-6}	-1.6×10^{-6}	-3.1×10^{-6}	-5.0×10^{-5}
ROA	2.8×10^{-4}	4.3×10^{-4}	-7.2×10^{-4}	-1.1×10^{-4}	6.4×10^{-5}	2.1×10^{-4}	1.2×10^{-4}

Typical experimental values were estimated from Refs. 68–76.

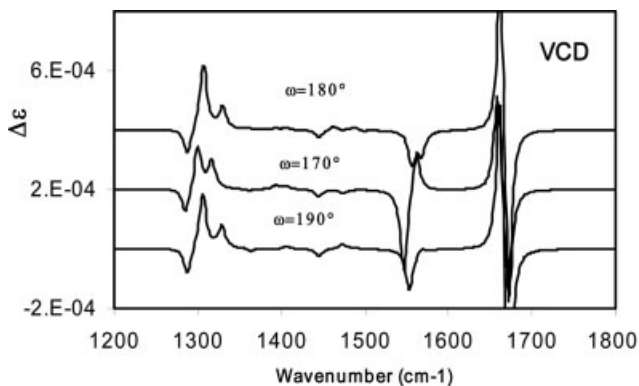


Fig. 12. Calculated (B3LYP/PCM/6-31G**) VCD intensities of the helical acetyl-L-alanyl-L-methylamide segment simulated with planar and nonplanar amide groups.

VCD. We tried to detect the amide I VCD in nonplanar cis-like polycyclic lactams, but without success (Malon and Keiderling, unpublished). The most important contribution from amide I bands would probably come from the frequency shift, which is quite significant. Amide I vibration also provides a very small ROA signal. The amide II and III vibrations are coupled with backbone protein and peptide vibrations, and interpretation of the spectra will likely be difficult. Still, the amide II and the amide III may be more hopeful regions where amide nonplanarity could be followed. In order to estimate probable nonplanarity contribution to peptide and protein VOA spectra, we compare the anisotropy ratios (“G-factors”),

$$G_{\text{ROA}} = \frac{I^{\text{R}} - I^{\text{L}}}{I^{\text{R}} + I^{\text{L}}} \quad \text{and} \quad G_{\text{VCD}} = \frac{\epsilon_{\text{L}} - \epsilon_{\text{R}}}{\epsilon_{\text{L}} + \epsilon_{\text{R}}},$$

calculated for selected NMA conformers to usual experimental values in Table 2. While the nonplanarity VCD contribution is at best only a small fraction of the usual values observed experimentally in peptides, the relative ROA contribution is much bigger. For example, for a relatively modest deformation of $\omega = 175^\circ$, the amide III internal nonplanarity ROA signal is comparable, and the amide I signal even seven times higher than the average values observed experimentally for proteins. This is rather surprising because until now this technique was not considered sensitive enough for distinguishing such local geometry features. The low wave number amide IV and amide V bands do not promise much hope in VCD, mainly for experimental reasons). However, they seem to have a large potential for nonplanar amide detection in Raman and ROA spectroscopy as recognized already by Polavarapu et al.³⁹ Clearly nonplanar amides should be visible in this region and measurements of standard protein structures using ROA below 1000 cm^{-1} should be a logical next step.

Until now the nonplanarity was discussed only for a very simple model, NMA. However, the topic has been already discussed for a bigger helical peptide segment previously acetylglycylmethylamide.³⁸ In this study, we per-

formed an analogous computation of acetyl-L-alanyl-L-methylamide. The molecule was kept in the α -helical conformation ($\varphi = -57^\circ$, $\psi = -47^\circ$) with the amide groups in planar ($\omega = 180^\circ$) and nonplanar ($\omega = 170^\circ$, 190°) conformations. These calculations agree with the previous results³⁸ and confirm the complexity of the interpretation of the amide III band and the coupling to the methyl hydrogen bending motion coupling. Moreover, the nonplanarity clearly modifies the VCD shape of the amide II band (Fig. 12) in favor of comparison with α -helical peptides.

Provided that the finding of MacArthur et al.⁶ is valid, i.e. the sense of the nonplanarity follows the main chain twist then for the α -helical (dextrorotatory) chains (trans-like amide— $\Delta\omega$ positive), our calculations predict ECD with negative $n-\pi^*$ band, amide I positive in VCD and negative in ROA, amide II negative in both VCD and ROA. The laevorotatory polyproline II type helix should analogously display all these signals with the reversed signs.

CONCLUSIONS

Our calculations explored various possibilities of optical spectroscopy techniques to detect and estimate the peptide bond nonplanarity. The nonplanarity causes significant changes namely in the ECD and the Raman optical activity spectra. With respect to eventual selective detection of the amide nonplanarity in peptides and proteins the Raman optical activity seems to be the most promising technique. ROA spectra combine a higher resolution of the vibrational spectroscopy with an enhanced sensitivity to local structure. The internal nonplanarity VCD and ECD signal may be less easy to detect due to the overlap with other factors and mechanisms moderating the spectral shapes. Most probably, simultaneous use of all the three chiroptical techniques (ECD, VCD and ROA) should provide enough markers for detection of the nonplanar amides even in complicated situations.

LITERATURE CITED

- Pauling L, Corey RB, Branson HR. Structure of proteins; two hydrogen bonded helical configurations of the polypeptide chain. *Proc Natl Acad Sci USA* 1951;37:205–211.
- Ramachandran GN, Sasisekharan V. Conformation of polypeptides and proteins. *Adv Prot Chem* 1968;28:283–437.
- Winkler F, Dunitz J. The non-planar amide group. *J Mol Biol* 1971;59:169–182.
- Ulmer TS, Ramirez BE, Delaglio F, Bax A. Evaluation of backbone proton positions and dynamics in a small protein by liquid crystal NMR spectroscopy. *J Am Chem Soc* 2003;125:9179–9191.
- Cerrini S, Gavuzzo E, Lucente G, Luisi G, Pinnen F, Radics L. Ten-membered cyclotriptides. III. Synthesis and conformation of cyclo(-Me beta Ala-Phe-Pro-) and cyclo(-Me beta Ala-Phe-DPro-). *Int J Pept Protein Res* 1991;38:289–297.
- MacArthur MW, Thornton JM. Deviations from planarity of the peptide bond in peptides and proteins. *J Mol Biol* 1996;264:1180–1195.
- Karplus PA. Experimentally observed conformation-dependent geometry and hidden strain in proteins. *Prot Sci* 1996;5:1406–1420.
- Esposito L, De Simone A, Zagari A, Vitagliano L. Correlation between omega and psi dihedral angles in protein structures. *J Mol Biol* 2005;347:483–487.
- Esposito L, Vitagliano L, Mazzarella L. Recent advances in atomic resolution protein crystallography. *Prot Pept Lett* 2002;9:95–106.

- Esposito L, Vitagliano L, Zagari A, Mazzarella L. Experimental evidence for the correlation of bond distances in peptide groups detected in ultrahigh-resolution protein structures. *Prot Eng* 2000;13:825–828.
- Sevcik J, Dauter Z, Lamzin VS, Wilson KS. Ribonuclease from *Streptomyces aureofaciens* at atomic resolution. *Acta Crystallogr D* 1996;52:327–344.
- Marquart M, Walter J, Deisenhofer J, Bode W, Huber R. The geometry of the reactive site and of the peptide groups in trypsin, trypsinogen and its complexes with inhibitors. *Acta Crystallogr B* 1983;39:480–490.
- Pierluigi C, Rondan N, G., Paddon-Row MN, Houk KN. Origin of r-facial stereoselectivity in additions to r-bonds: generality of the anti-periplanar effect. *J Am Chem Soc* 1981;103:2438–2440.
- Ramachandran GN, Kolaskar AS. The non-planar peptide unit. II. Comparison of theory with crystal structure data. *Biochim Biophys Acta* 1973;303:385–388.
- Ramachandran GN, Lakshminarayanan AV, Kolaskar AS. Theory of the non-planar peptide unit. *Biochim Biophys Acta* 1973;303:8–13.
- Warshel A, Levitt M, Lifson S. Consistent force field for calculation of vibrational spectra and conformations of some amides and lactam rings. *J Mol Spectrosc* 1970;33:84–99.
- Sulzbach HM, Schleyer PR, Schaefer HF. Influence of the nonplanarity of the amide moiety on computed chemical shifts in peptide analogs. Is the amide nitrogen pyramidal? *J Am Chem Soc* 1995;117:2632–2637.
- Hu JS, Bax A. Determination of ϕ and χ_1 angles in proteins from ^{13}C - ^{13}C three-bond J couplings measured by three-dimensional heteronuclear NMR. How planar is the peptide bond? *J Am Chem Soc* 1997;119:6360–6368.
- Cieplak AS. Solid-state conformations of linear oligopeptides and aliphatic amides. A model of chiral perturbation of a conjugated system. *J Am Chem Soc* 1985;107:271–273.
- Esposito L, Vitagliano L, Zagari A, Mazzarella L. Pyramidalization of backbone carbonyl carbon atoms in proteins. *Prot Sci* 2000;9:2038–2042.
- Parker FS. Applications of infrared, Raman and resonance Raman spectroscopy. New York: Plenum; 1983.
- Nafie LA, Yu GS, Qu X, Freedman TB. Comparison of IR and Raman forms of vibrational optical activity. *Faraday Discuss* 1994;99:13–34.
- Bussian BM, Sander C. How to determine protein secondary structure in solution by Raman spectroscopy: practical guide and test case DNase I. *Biochemistry* 1989;28:4271–4277.
- Tu AT. Raman spectroscopy in biology. New York: Wiley; 1982.
- McClure WF, Maeda H, Dong J, Liu Y, Ozaki Y. Two-dimensional correlation of Fourier transform near-infrared and Fourier transform Raman spectra I: mixtures of sugar and protein. *Appl Spectrosc* 1996;50:467–475.
- Bláha K, Farag AM, Vanderhelm D, Hossain MB, Buděšínský M, Maloň P, Smolíková J, Tichý M. Stereoisomeric chiral 2,9-diazabicyclo[4.4.0]decane-3,10-diones as model of dipeptide grouping: synthesis, X-Ray, IR, NMR and CD studies. *Collect Czech Chem Commun* 1984;49:712–718.
- Smolíková J, Tichý M, Bláha K. Infrared spectroscopy of 4-azatricyclo[4.4.0,0]decan-5-one- α -lactam with a nonplanar cis-amide group. *Collect Czech Chem Commun* 1976;41:413–428.
- Maloň P, Frič I, Tichý M, Bláha K. Chiroptical properties of (–)-4-methyl-4-azatricyclo[4.4.0,0]decan-5-one- α -lactam with a nonplanar tertiary cis-amide group. *Collect Czech Chem Commun* 1977;42:3104–3100.
- Frič I, Maloň P, Tichý M, Bláha K. Chiroptical properties of 4-azatricyclo[4.4.0,0]decan-5-one- α -lactam with a nonplanar cis-amide group. *Collect Czech Chem Commun* 1977;42:678–690.
- Tichý M, Maloň P, Frič I, Bláha K. Synthesis and chiroptical properties of (–)-(1R)-3-azatricyclo[5.4.0,0]undecan-2-one- α -lactam with non-planar cis-amide group. *Collect Czech Chem Commun* 1979;44:2653–2659.
- Tvaroška I, Bystrický S, Maloň P, Bláha K. Nonplanar conformation of *N*-methylacetamide: Solvent effect and chiroptical properties. *Collect Czech Chem Commun* 1982;47:17–28.
- Maloň P, Bláha K. Quantum chemical calculations on 4-aza-4-tricyclo[4.4.4.0]decan-5-one- α -lactam with non-planar cis-amide group. *Collect Czech Chem Commun* 1977;42:687–696.
- Baumruk V, Pančoška P, Keiderling TA. Predictions of secondary structure using statistical analyses of electronic and vibrational circular dichroism and Fourier transform infrared spectra of proteins in H_2O . *J Mol Biol* 1996;259:774–791.
- Keiderling TA. Vibrational Circular Dichroism. Comparison of technique and practical considerations. In: Krishnan K, Ferraro JR, editors. *Practical Fourier transform infrared spectroscopy*. San Diego: Academic Press; 1990. p 203–284.
- Keiderling TA. Protein structural studies using vibrational circular dichroism spectroscopy. In: Havel H, editor. *Spectroscopic methods for determining protein structure in solution*. New York: VCH Publishers; 1995. p 163–169.
- Barron LD, Hecht L, Bell AD. Vibrational Raman optical activity of biomolecules. In: Fasman GD, editor. *Circular dichroism and the conformational analysis of biomolecules*. New York: Plenum; 1996. p 653–695.
- Barron LD, Ford SJ, Bell AD, Wilson G, Hecht L, Cooper A. Vibrational Raman optical activity of biopolymers. *Faraday Discuss* 1994;99:217–232.
- Maloň P, Bouř P. Amide group non-planarity in helical peptide segments: vibrational optical activity implications. In: Maia HLS, editor. *Peptides 1994*, Leiden; 1994. p 513–514.
- Polavarapu PL, Deng ZY, Ewig CS. Vibrational properties of the peptide group—Achiral and chiral conformers of *N*-methyl acetamide. *J Phys Chem* 1994;98:9919–9930.
- Rick SW, Cachau RE. The nonplanarity of the peptide group: molecular dynamics simulations with a polarizable two-state model for the peptide bond. *J Chem Phys* 2000;112:5230–5241.
- Selvarengan P, Kolaival P. Study of nonplanarity of peptide bond using theoretical calculations. *Bioorg Chem* 2005;33:253–263.
- Frisch MJ, Trucks GW, Schlegel HB, Scuseria GE, Robb MA, Cheeseman JR, Montgomery JA, Vreven JT, Kudin KN, Burant JC, et al. *Gaussian 03*. Pittsburgh, PA: Gaussian, Inc.; 2003.
- Becke AD. A multicenter numerical integration scheme for polyatomic molecules. *J Chem Phys* 1988;88:2547–2553.
- Becke AD. Exchange-correlation approximations in density-functional theory. In: Yarkony DR, editor. *Modern electronic structure theory*, Vol. 2. Singapore: World Scientific; 1995. p 1022–1046.
- Møller C, Plesset MS. Note on an approximation treatment for many-electron systems. *Phys Rev* 1934;46:618–622.
- Bouř P, Sopková J, Bednářová L, Maloň P, Keiderling TA. Transfer of molecular property tensors in Cartesian coordinates: a new algorithm for simulation of vibrational spectra. *J Comput Chem* 1997;18:646–659.
- Bouř P, Baumruk V, Hanzlíková J. Measurement and calculation of the Raman optical activity of alpha-pinene and *trans*-pinane. *Collect Czech Chem Commun* 1997;62:1384–1395.
- Bouř P. Computations of the Raman optical activity via the sum-over-states expansions. *J Comput Chem* 2001;22:426–435.
- Stephens PJ, Devlin FJ, Ashvar CS, Chabalowski CF, Frisch MJ. Theoretical calculation of vibrational circular dichroism spectra. *Faraday Discuss* 1994;99:103–119.
- Ruud K, Helgaker T, Bouř P. Gauge-origin independent density-functional theory calculations of vibrational Raman optical activity. *J Phys Chem A* 2002;106:7448–7455.
- Furche F, Alhrichs R. Time-dependent density functional methods for excited state properties. *J Chem Phys* 2004;121:12772–12773.
- Schroeder OE, Carper E, Wind JJ, Poutsma JL, Etkorn FA, Poutsma JC. Theoretical and experimental investigation of the energetics of *cis-trans* proline isomerization in peptide models. *J Phys Chem A* 2006;110:6522–6530.
- Mennucci B, Martinez J. How to model solvation of peptides? Insights from a quantum-mechanical and molecular dynamics study of *N*-methylacetamide. 1. Geometries, infrared, and ultraviolet spectra in water. *J Phys Chem B Condens Matter Mater Surf Interf Biophys* 2005;109:9818–9829.

54. Gaigeot MP, Sprik M, Vuilleumier R, Borgis D. Infrared spectroscopy of *N*-methylacetamide revisited by ab initio dynamic simulations. *J Chem Theor Comp* 2005;1:772–789.
55. Basch H, Robin MB, A. KN. Electronic states of the amide group. *J Chem Phys* 1967;47:1201–1210.
56. Basch H, Robin MB, Kuebler NA. Electronic spectra of isoelectronic amides, acids, and acyl fluorides. *J Chem Phys* 1968;49:5007–5018.
57. Boyd DB, Riehl JP, Richardson FS. Chiroptical properties of 1-carbapenam and orbital mixing in nonplanar amides. *Tetrahedron* 1979;35:1499–1508.
58. Clayden J, Moran WJ. The twisted amide 2-quinuclidone: 60 years in the making. *Angew Chem Int Ed Engl* 2006;45:7118–7120.
59. Sznatke G. Semiempirical rules in circular dichroism of natural products. *Pure Appl Chem* 1979;51:769–785.
60. Fasman GD. In: Fasman GD, editor. *Circular dichroism and the conformational analysis of biomolecules*. New York: Plenum; 1996.
61. Merritt EA, Kuhn P, Sarfaty S, Erbe JL, Holmes RK, Hol WG. The 1.25 Å resolution refinement of the cholera toxin B-pentamer: evidence of peptide backbone strain at the receptor-binding site. *J Mol Biol* 1998;282:1043–1059.
62. Šebek J, Kejlik Z, Bouř P. Geometry and solvent dependence of the electronic spectra of the amide group and consequences for peptide circular dichroism. *J Phys Chem A* 2006;110:4702–4711.
63. Kubelka J, Keiderling TA. Differentiation of β -sheet forming structures: Ab initio based simulations of IR absorption and vibrational CD for model peptide and protein β -sheets. *J Am Chem Soc* 2001;123:12048–12058.
64. Song S, Asher SA, Krimm S. Assignment of a new conformation-sensitive UV resonance Raman band in peptides and proteins. *J Am Chem Soc* 1988;110:8547–8548.
65. Song S, Asher SA, Krimm S. Ultraviolet resonance Raman studies of trans and cis peptides: photochemical consequences of the twisted p excited state. *J Am Chem Soc* 1991;113:1155–1163.
66. Asher SA, Li P, Chi ZH, Chen XG, Schweitzer-Stenner R, Mirkin NG, Krimm S. Vibrational assignments of *trans-N*-methylacetamide and some of its deuterated isotopomers from band decomposition of IR, visible, and resonance Raman spectra—Comment—Reply. *J Phys Chem* 1997;101:3992–3994.
67. Chen XG, Schweitzer-Stenner R, Asher SA, Mirkin NG, Krimm S. Vibrational assignments of *trans-N*-methylacetamide and some of its deuterated isotopomers from band decomposition of IR, visible, and resonance Raman spectra. *J Phys Chem* 1995;99:3074–3083.
68. Keiderling TA. Protein and peptide secondary structure and conformational determination with vibrational circular dichroism. *Curr Opin Chem Biol* 2002;6:682–688.
69. Keiderling TA. Vibrational circular dichroism applications to conformational analysis of biomolecules. In: Fasman GD, editor. *Circular dichroism and the conformational analysis of biomolecules*. New York: Plenum; 1996. p 555–598.
70. Pančoška P, Janota V, Nešetřil J. Novel matrix descriptor for determination of the connectivity of secondary structure segments in proteins. Analysis of general properties using graph theory. *Discret Math* 2001;235:399–423.
71. Eker F, Cao X, Nafie L, Schweitzer-Stenner R. Tripeptides adopt stable structures in water. A combined polarized visible Raman, FTIR, and VCD spectroscopy study. *J Am Chem Soc* 2002;124:14330–14341.
72. McColl IH, Blanch EW, Gill AC, Rhie AGO, Ritchie MA, Hecht L, Nielsen K, Barron LD. A new perspective on beta-sheet structures using vibrational Raman optical activity: From poly(L-lysine) to the prion protein. *J Am Chem Soc* 2003;125:10019–10026.
73. Armand P, Kirschenbaum K, Goldsmith RA, Farr-Jones S, Barron AE, Truong KTV, Dill KA, Mierke DF, Cohem FE, Zuckermann RN, et al. NMR determination of the major solution conformation of a peptoid pentamer with chiral side chains. *Proc Natl Acad Sci USA* 1998;95:4309–4314.
74. McColl IH, Blanch EW, Hecht L, Barron LD. A study of alpha-helix hydration in polypeptides, proteins, and viruses using vibrational Raman optical activity. *J Am Chem Soc* 2004;126:8181–8188.
75. Keiderling TA, Kubelka J, Hilario J. Vibrational circular dichroism of biopolymers. Summary of methods and applications. In: Braiman M, Gregoriou V, editors. *Vibrational spectroscopy of polymers and biological systems*. Amsterdam–New York: Marcel Dekker; 2005.
76. Zhao C, Polavarapu PL, Das C, Balaram P. Vibrational circular dichroism of β -hairpin peptides. *J Am Chem Soc* 2000;122:8228–8231.